Shrinkage Cracking Characteristics of Compacted Fine-Grained Soils

H. Al-Dakheeli & R. Bulut
School of Civil and Environmental Engineering, Oklahoma State University, Stillwater, OK 74078, USA

ABSTRACT: Shrinkage cracking influences the functionality of compacted soils in geotechnical and geoenvironmental engineering applications. It can decrease the soil strength and increase the hydraulic conductivity. Despite of its significance, little attention has been given to study the characteristics of cracking in compacted soils. This research studies the relation between the soil cracking and shrinkage strain of compacted soils in the laboratory. To achieve that, restrained shrinkage tests have been conducted for expansive soils compacted close to the optimum moisture content and subjected to the air drying. The restrained shrinkage is carried out using the restrained ring testing method. The volume change for all the tests is estimated by the digital image processing technique. In addition to the shrinkage strain and cracks, soil suction is also tracked during the drying process. For all the tested specimens, a single crack initiates at the inner face of the circular-hole specimens and grows toward the exterior edge. Based on the soil shrinkage curve, it is found that crack initiation occurs after the soil specimens accomplish the normal shrinkage and commences the residual shrinkage stage. However, this stage varies for the specimens of the same soil depending on the initial water content of the compacted specimens. The crack keeps growing in width until the water content hits the shrinkage limit.

1 INTRODUCTION

The compacted soils are widely utilized for the applications of geotechnical and geoenvironmental engineering. The drying shrinkage on these soils can lead to cracking of those layers. Cracks can substantially decrease the strength and increase the compressibility and permeability (Morris et al., 1992). The existence of cracks in the soil layers utilized for the environmental sealing purposes can result in losing their functions (Peron et al., 2009). The presence of cracks in pavement shoulders can extend the seasonal moisture variation and hence subject the subgrades to more movements. In extreme conditions, cracks can initiate in the subgrade and may propagate to cause longitudinal cracks in the pavement layers. Such cases have widely been reported (Lytton et al., 2005; Luo and Prozzi, 2009; Bulut et. al., 2014; Wanyan et. al., 2015; Nevels et al., 2016).

Due to the complexity behind the drying cracking phenomenon in the soil, understanding its mechanism bears on significant difficulty. However, some experimental results may make it possible to define some characteristics of drying soil cracking. Various studies have investigated the crack initiation in initially saturated soils subjected to desiccation conditions. After developing some shrinkage, most of these studies have shown the cracks initiated in the tested soils when the suction becomes close to the air entry value (Lloret et al., 1998; Nahlawi and Kodikara, 2006; Rodríguez et al., 2007; Peron et al., 2009; Shin and Santamarina, 2011; Shannon et al., 2015; Saleh-Mbemba et al., 2016). This paper attempts to extend this observation in the literature to involve the initially compacted unsaturated soils by relying on the soil shrinkage curve (SSC).

The typical SSC, gravimetric water content versus void ratio, for slurry soils consists of three zones: normal shrinkage, residual shrinkage, and zero shrinkage (Fig. 1).

However, for initially unsaturated soils, particularly the compacted soils, a structural shrinkage may take place prior to the normal shrinkage (Fig. 2) (Li et al., 2014). The SSC of initially saturated soils and initially unsaturated compacted soils indicates that the normal shrinkage is highly linear. Besides, the soil experiences the most shrinkage during the normal shrinkage zone.

The air entry stage occurs for initially saturated soils at the end of the normal shrinkage. The end of the normal shrinkage for initially unsaturated soils may also represent the air entry stage, especially for the micropores, but not for the overall soil mass (Fityus and Buzzi, 2009). Based on that, a question is asked: do the cracks initiate at the end of the nor-

mal shrinkage (i.e., the stage of air entry through the micropores)?

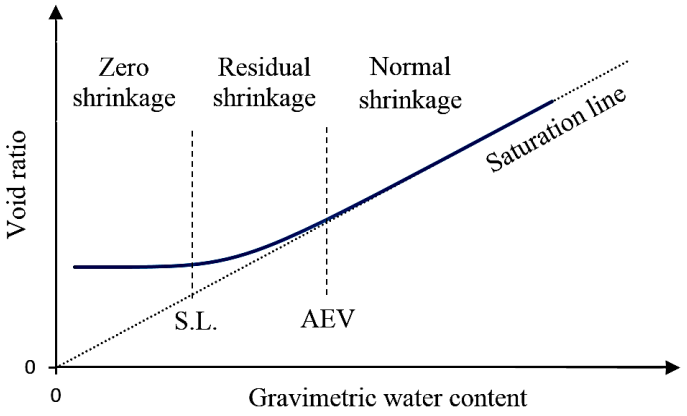

Figure 1. Typical shrinkage curve for initially slurry soil, AEV: air entry value, S.L.: shrinkage limit.

This paper employs results from restrained ring tests (RRT) for soils collected from Oklahoma to answer this question. Compacted circular-hole specimens in RRT are exposed to air drying. During desiccation, the soil experiences shrinkage and eventually cracks. The shrinkage of the soil surface is evaluated using digital image analysis technique by utilizing images captured by a high-resolution camera fixed on the top of the specimens. The results confirm that the soil first cracks when the shrinkage completes the linear tendency.

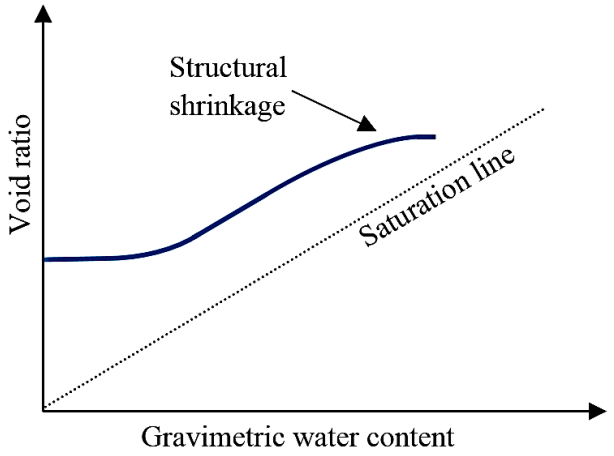

Figure 2. Typical shrinkage curve for structural soil (e.g. compacted and undisturbed soils) (Cornelis et al., 2006).

2 SOIL MATERIAL AND ITS PROPERTIES

The soils tested in this study were obtained from Ardmore and Lake Hefner in Oklahoma using the push-tube sampling. They were broken into pieces, air-dried and further broken into much smaller sizes. The basic geotechnical properties of this soil were obtained by following the relevant ASTM standards and the results are given in Table 1.

Table 1. Basic geotechnical properties of tested soils.

Soil property	Ardmore	Lake Hefner
Clay content (%)	40	30
Silt content (%)	47	54
Fine sand content (%)	13	16
Plastic limit (%)	24	15
Liquid limit (%)	55	29
Optimum water content (%)	26.5	15
Maximum dry density (g/cm^3)	1.46	1.82

3 LABORATORY TESTS

3.1 *Restrained Ring Test*

The RRT is a testing technique in which the soil is restrained from shrinking freely as it is subjected to desiccation conditions. It has been used to study the drying cracking in the soils by Abou Najm et al. (2009), Chen (2015), and Shannon et al. (2015).

The restrained ring test (RRT) was conducted on circular-hole specimens with 5.5 cm in inner diameter, 15.24 cm in external diameter, and 1.65 cm in thickness (Fig. 3). The specimen was prepared by moulding soil inside a PVC ring with the same external diameter. The specimens were prepared by compacting the soil inside the PVC ring in two layers with each layer receiving 36 blows using a wooden rod with rubber cab (diameter = 2.54 cm). With the help of a sharp edge steel cylinder, 5.5 cm in diameter, a hole in the sample core was made by pushing the sharp edge steel cylinder through the core of the specimens. The obtained soil specimen was sealed and stored in an ice-chest for curing and suction equilibrium for one week. Before starting the test, a PVC ring with 5.5 cm in outer diameter was gently pushed inside the hole in the core of the specimen. Before starting the test, the soil specimen was sealed by plastic wrap from the bottom and a rubber band from the circumference to maintain the sealing for uniform shrinkage as the soil sample shrinks radially. Attention was given to prevent the rubber band from applying any pressure on the soil by keeping it loose and for sealing purpose only.

A camera was fixed for the top view of the specimens to capture digital still images for the specimens during shrinkage and drying process. It was set to take a single image every 15 minutes. The obtained images were analysed to estimate the shrinkage strain using digital image analysis technique. The digital image analysis was carried out in MATLAB using *GeoPIV-RG* subroutines. Information about the background and the theory involved in these software subroutines can be found in White et al. (2003) and Stanier et al. (2016). Small white sand particles were spread randomly on the specimen sur-

face to capture the displacement of the surface specimen calculated by *GeoPIV-RG* (Fig. 3).

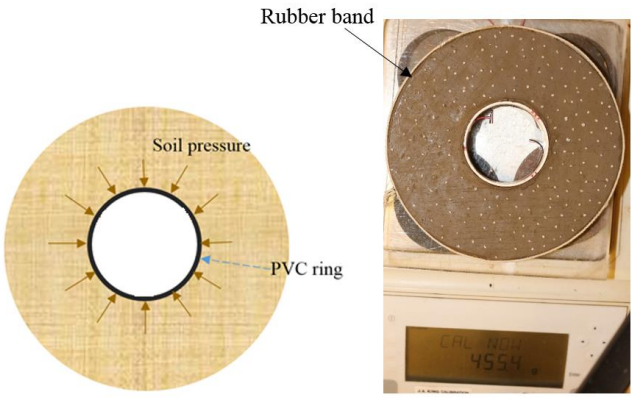

Figure 3. Soil specimen in Restrained Ring Test.

The soil suction was measured independently on the representative specimens using the WP4 device and tensiometer sensor. In the study, it was assumed that the osmotic suction component is negligible.

4 RESULTS

The suction measurements are fitted by the Fredlund and Xing (1994) model for both compacted soils and are depicted in Figure 4. After starting the test, specimens in the restrained ring test (RRT) develop radial shrinkage toward the core PVC ring. All the specimens tested by RRT evolve a single crack initiated at the inner edge and the crack grows toward the exterior face (Figures 5a and 5b). This crack grows in width as well. However, at a certain stage, the crack width becomes stable (Figure 5c). It is believed that the water content at this stage attains the shrinkage limit at which the shrinkage ceases. In order to evaluate whether the crack initiation occurs at the end of the normal shrinkage, two-dimensional surface shrinkage strains were computed, and the results were plotted against the gravimetric water content (i.e., 2D strain-*w* curve) in Figure 6. The *GeoPIV-RG* subroutines can directly compute the strain in the specimen surface area by dividing the desired area into meshes or patches. The surface shrinkage strain is obtained from the ratio between the reduction of the area and the original area for patches in every image, as compared to the chosen original image (e.g., first image captured during the test). Since only a single crack developed, it was not difficult to evaluate the soil shrinkage for the specimens after the crack initiation. A simple approach was carried out by eliminating the crack area and computing the shrinkage for the uncracked area only. Although the volumetric shrinkage is not assessed since the shrinkage in the specimen thickness is not measured, it is still possible to identify the normal shrinkage boundaries from the 2D strain-*w* curve. This can be carried out by locating the linear portion in the 2D strain-*w* curve.

The 2D strain-*w* curve for the specimens of Ardmore and Lake Hefner soil is shown in Figure 6.

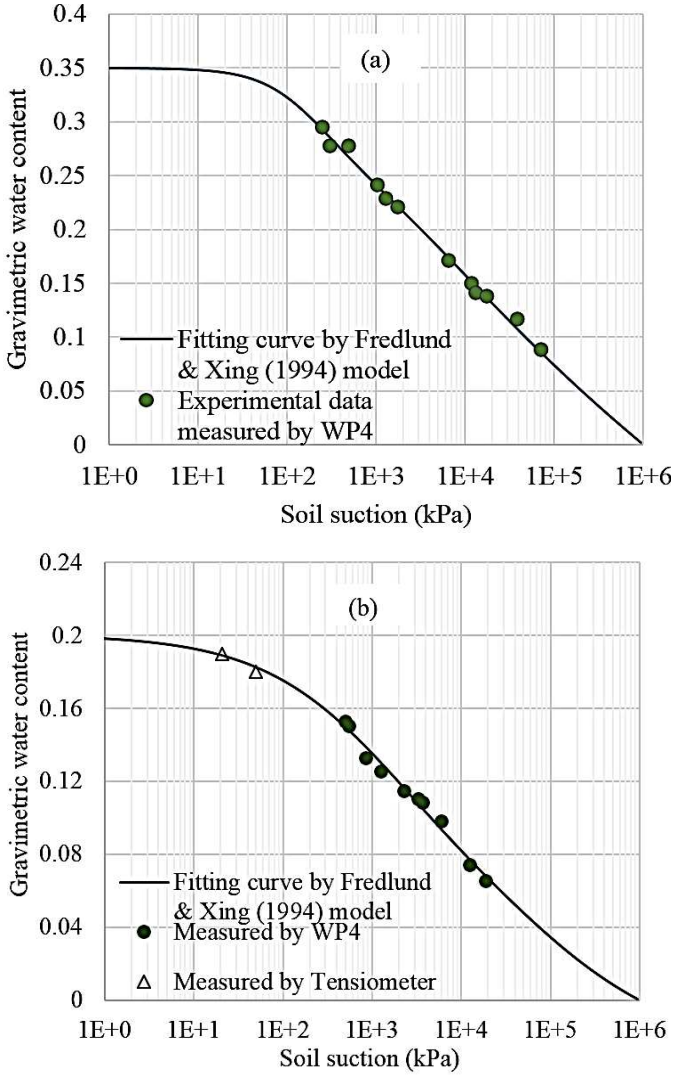

Figure 4. Soil water characteristic curve for: (a) Ardmore soil, (b) Lake Hefner.

The results of suction versus 2D shrinkage strain for the tested specimens are drawn in Figure 7. Specimens of Ardmore soil with initial gravimetric water content (*w*) 30.7% and 26.1% crack at *w* equal to 22.1% and 20.2%, respectively. Specimens of Lake Hefner soil with initial *w* 20.1% and 16.1% crack at *w* equal to 14.1% and 11.6%, respectively. The results are summarized in Table 2. From Figure 6, the *w* of crack initiation falls close to the end of the linear portion once the shrinkage is hindering and deviating from the linear tendency. That happens for all the tested specimens of both soil types (Table 1). As aforementioned, the end of the linear curve is also the end of the normal shrinkage and the beginning of the residual shrinkage zone. However, this stage varies for different initial water contents, w_i, of the compacted soil. This may be attributed to the variation of the macro-pores distribution depending on the w_i, since the macro-pores are predominant in the compacted soils (Jayawickrama and Lytton, 1993).

Therefore, the shrinkage and cracking characteristics such as the shrinkage magnitude before cracking, stage of crack initiation and crack growth magnitude, should be evaluated for representative samples (e.g., undisturbed samples).

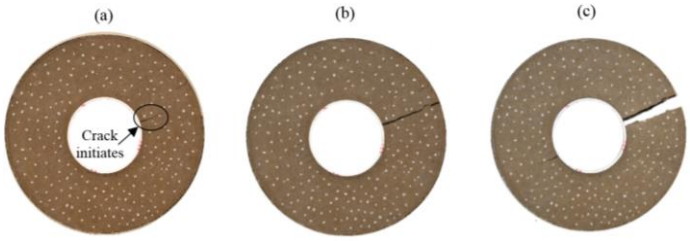

Figure 5. Stages of crack initiation and growth for Ardmore soil specimen with initial w equal to 30.7%, (a) w =22.1%, (b) w =19.8%, (c) w =13.9%.

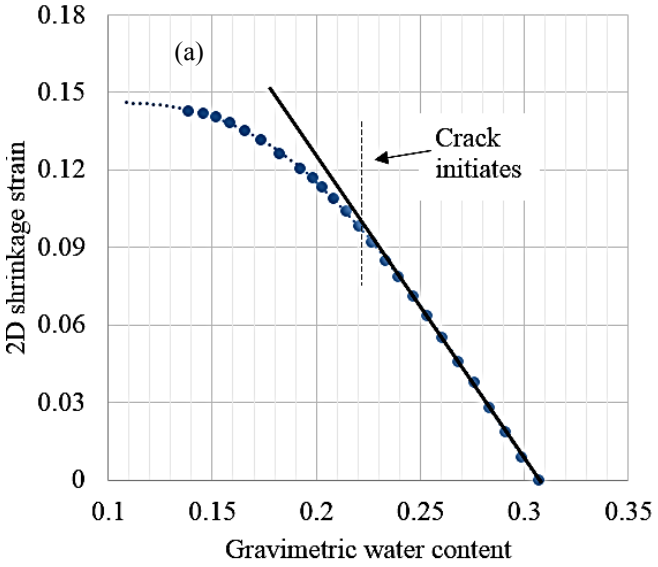

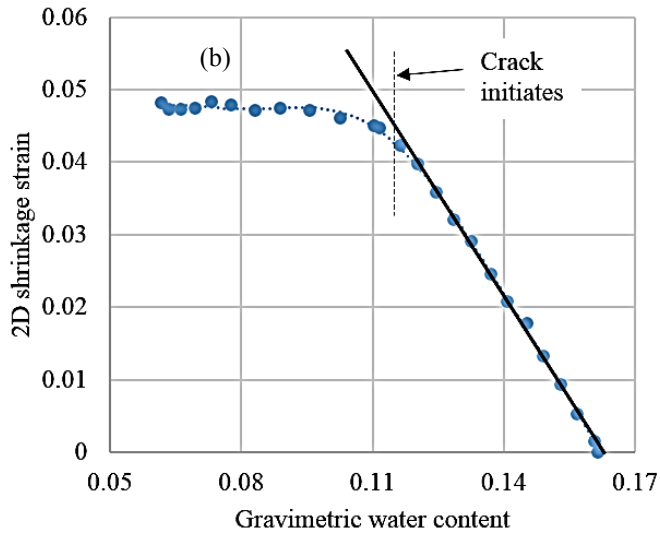

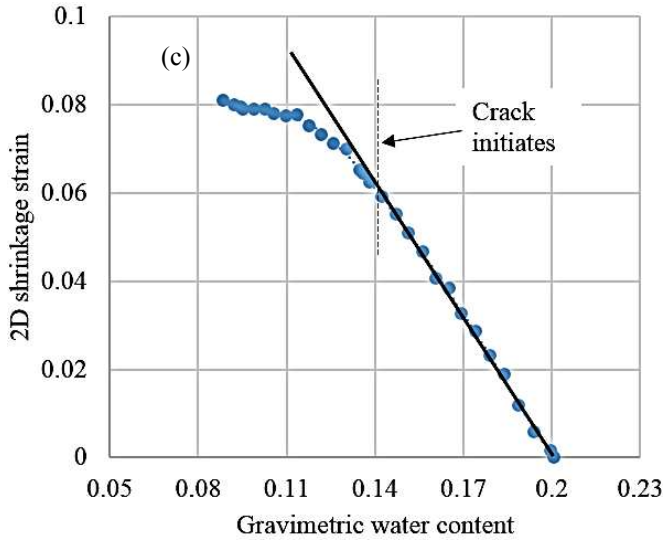

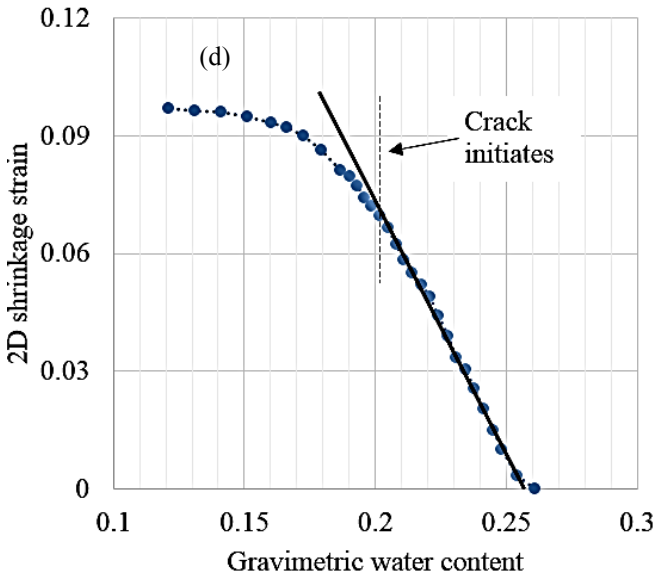

Figure 6. Shrinkage strain-w curve for the specimens of Ardmore and Lake Hefner soil: (a) Ardmore, w_i =30.7%, (b) Ardmore, w_i =26.1%, (c) Lake Hefner, w_i =20.1%, (d) Lake Hefner, w_i =16.1%.

For the 2D strain-suction curve (Fig. 7), the boundaries of the normal shrinkage are not clear. This is because the 2D strain-suction curve keeps somehow linear even beyond the end of the normal shrinkage zone (Fig. 7). Another note on the results is that a small amount of structural shrinkage has been seen for one specimen of the Ardmore soil (Fig. 6b). This happens perhaps because this specimen was compacted with water slightly drier than the optimum moisture (Sheng et al., 2013).

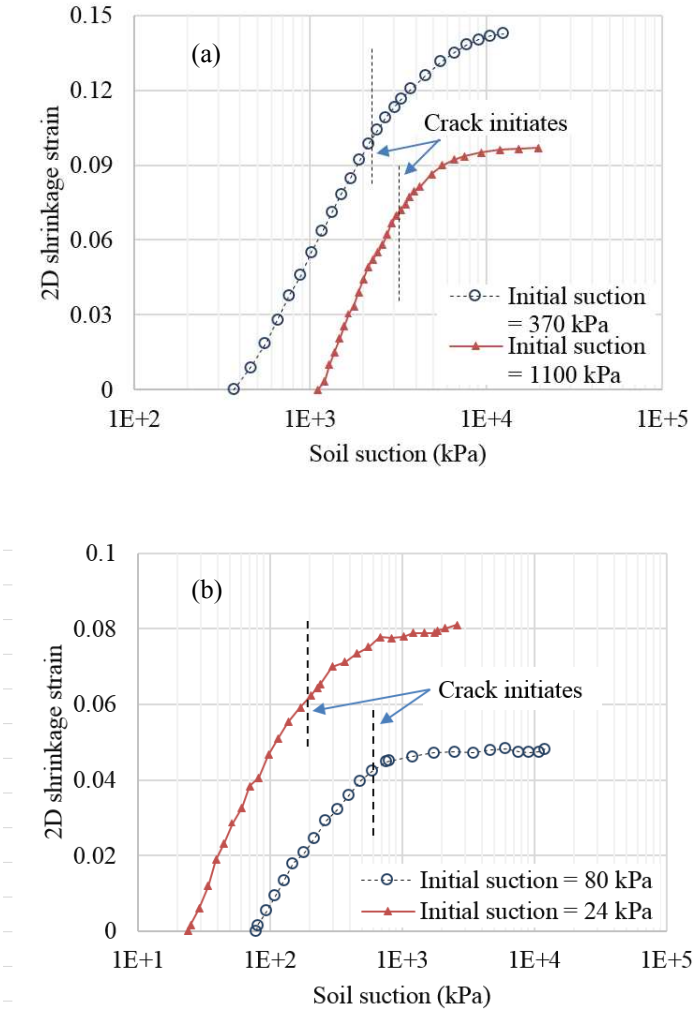

Figure 7. Shrinkage strain-suction curve for the specimens of (a) Ardmore soil, (b) Lake Hefner soil.

Table 2. Summary of initial conditions and crack initiation water content of tested soils.

Soil	Initial w (%)	Initial dry density (gm/cm^3)	w at crack initiation stage (%)
Ardmore	30.7	1.46	22.1
	26.1	1.56	20.2
Lake Hefner	20.1	1.81	14.1
	16.1	1.90	11.6

5 CONCLUSIONS

While the mechanism of the soil shrinkage cracking for compacted soils is highly complex, experimental results may help to identify some of its characteristics. Studies have shown that drying of initially slurry expansive soils in the laboratory starts generating cracks at suction close to the air entry value (AEV). From the typical non-structural shrinkage curve, the air entry occurs when the soil shrinkage just deviates from the linear tendency or when the normal shrinkage is completely exhausted. In this research, compacted specimens of the soils from Oklahoma are tested using the restrained ring testing method. While drying, shrinkage magnitude is evaluated as an attempt to examine whether the crack initiation for compacted specimens also happens at the end of the linear normal shrinkage zone. The uniqueness of the restrained ring test is that the shrinkage of the specimen develops a single crack only in most cases. The shrinkage is estimated for the surface of the circular-hole specimens in two dimensions only. However, identifying the normal shrinkage boundaries was possible by locating the linear portion of the shrinkage strain versus gravimetric water content curve. For all the tested specimens of both soils, the crack initiates when the shrinkage becomes close to the end of normal shrinkage. However, for different initial water contents, the end of the linear normal shrinkage zone occurs also at different water contents. Therefore, the crack initiation of the specimens happens at different water contents for the same soil but different initial water content. Hence, it is recommended to evaluate the crack initiation by testing representative specimens.

6 REFERENCES

Abou Najm, M., Mohtar, R.H., Weiss, J. & Braudeau, E. 2009. Assessing internal stress evolution in unsaturated soils. *Water Resources Research* 45(5).

Bulut, R., Chen, L.Z., Mantri, S., Amer, O., Tian, Y. & Zaman, M. 2014. Drying shrinkage problems in high PI subgrade soils. *ODOT SP&R Item Number 2236*. Oklahoma.

Chen, L. 2015. Development of a new tensile stress model for expansive soils. *Ph.D. Dissertation. Oklahoma State University, Oklahoma*.

Cornelis, W.M., Corluy, J., Medina, H., Diaz, J., Hartmann, R., Van Meirvenne, M. & Ruiz, M.E. 2006. Measuring and modelling the soil shrinkage characteristic curve. *Geoderma* 137(1): 179-191.

Fityus, S. & Buzzi, O. 2009. The place of expansive clays in the framework of unsaturated soil mechanics. *Applied Clay Science* 43(2): 150-155.

Fredlund, D.G. & Xing, A. 1994. Equations for the soil-water characteristic curve. *Canadian Geotechnical Journal* 31(4): 521-532.

Jayawickrama, P.W. & Lytton, R.L. 1993. Conductivity through macropores in compacted clays. In: ASCE Geotechnical Division (Ed.), *7th International Conference on Expansive Soils*, Dallas, Texas: 99–104.

Li, X., Zhang, L.M. & Wu, L.Z. 2014. A framework for unifying soil fabric, suction, void ratio, and water content during the dehydration process. *Soil Science Society of America Journal* 78(2): 387-399.

Lloret, A., Ledesma, A., Rodriguez, R., Sanchez, M.J., Olivella, S. & Suriol, J. 1998. Crack initiation in drying soils. Unsaturated Soils, P´ekin, *International Academic Publishers*: 497–502.

Luo, R. & Prozzi, J. 2009. Combining geogrid reinforcement and lime treatment to control dry land longitudinal cracking. *Transportation Research Record: Journal of the Transportation Research Board* 2104: 88-96.

Lytton, R.L., Aubeny, C.P. & Bulut, R. 2005. Design procedure for pavements on expansive soils. *Research Report No. FHWA/TX-05/0-4518-1, Vol. 1, Texas Transportation Institute, The Texas A&M University System, College Station, Texas*: 198.

Morris, P.H., Graham, J. & Williams, D.J. 1992. Cracking in drying soils. *Canadian Geotechnical Journal* 29(2): 263-277.

Nahlawi, H. & Kodikara, J.K. 2006. Laboratory experiments on desiccation cracking of thin soil layers. *Geotechnical and Geological Engineering* 24: 1641–1664.

Nevels Jr, J.B., Clarke, C.R., Chen, L. & Bulut, R. 2016. A site assessment of pavement cracking in a drought environment: a case history. In *E3S Web of Conferences* 9. EDP Sciences.

Peron, H., Laloui, L., Hueckel, T. & Hu, L.B. 2009. Desiccation cracking of soils. *European Journal of Environmental and Civil Engineering* 13(7-8): 869-888.

Rodríguez, R., Sanchez, M., Ledesma, A. & Lloret, A. 2007. Experimental and numerical analysis of desiccation of a mining waste. *Canadian Geotechnical Journal* 44(6): 644-658.

Saleh-Mbemba, F., Aubertin, M., Mbonimpa, M. & Li, L. 2016. Experimental characterization of the shrinkage and water retention behaviour of tailings from hard rock mines. *Geotechnical and Geological Engineering 34*(1): 251-266.

Shannon, B., Kodikara, J. & Pathmanathan, R. 2015. The use of restrained ring test method for soil desiccation studies. *Geotechnical Testing Journal [P]* 38(1): 98-112.

Sheng, D., Zhang, S. & Yu, Z. 2013. Unanswered questions in unsaturated soil mechanics. *Sci. China Technological Sciences* 56(5): 1257-1272.

Shin, H. & Santamarina, J.C. 2011. Desiccation cracks in saturated fine-grained soils: particle level phenomena and effective-stress analysis. *Géotechnique* 61(11): 961.

Stanier, S.A., Blaber, J., Take, W.A. & White, D.J. 2016. Improved image-based deformation measurement for geotechnical applications. *Canadian Geotechnical Journal* 53.

Wanyan, Y., Abdallah, I., Nazarian, S. & Puppala, A.J. 2014. Moisture content-based longitudinal cracking prediction and evaluation model for low-volume roads over expansive soils. *Journal of Materials in Civil Engineering* 27(10): 04014263.

White, D.J., Take, W.A. & Bolton, M.D. 2003. Soil deformation measurement using particle image velocimetry (PIV) and photogrammetry. *Geotechnique* 53(7): 619-631.